On the fixed-time control of systems with mismatched perturbations: An application to Quadrotor Unmanned Aerial Vehicles

Marco A. Arteaga, *UNAM*, Mexico
Javier Pliego-Jiménez, *CICESE*, Ensenada, Mexico
Emmanuel Moulay, *Université de Poitiers*, France
Michael Defoort, *University Polytechnic Hauts-de-France*

***Abstract*—Quadrotor Unmanned Aerial Vehicles (QUAVs) have become increasingly important in the recent years due to their potential in several industrial and social applications. Control design for this kind of nonlinear systems is a challenging task due to their under-actuated nature, where the position and attitude subsystems are highly coupled, and the fact that attitude states evolve on a non-Euclidean manifold. In this paper, a general solution is proposed to fully reject matched and mismatched perturbations under some usual assumptions, and the result is adapted for the fixed-time control of QUAVs. The scheme is shown to be singularity free, both for the sliding mode surface and for the orientation control term. The theory is tested through numerical simulations.**

***Index Terms*—Quadrotor Unmanned Aerial Vehicles, fixed-time stability, disturbance rejection, position tracking.**

I. Introduction

Unmanned Aerial Vehicles (UAVs), particularly quadrators, have become increasingly important in the recent years due to their potential in several industrial and social applications [1]. Quadrotors have a very simple mechanical structure with four rotors allowing them to perform hovering along with Vertical Take-Off and Landing (VTOL) maneuvers, although they are under-actuated and highly nonlinear systems [2].

Proportional-Integral-Derivative (PID) controllers have been successfully applied to quadrotors; however, for applications that require aggressive maneuvers or in the presence of external disturbances, these controllers exhibit large steady state errors [3]. Several control techniques have been explored to design trajectory tracking control laws for UAVs, including backstepping [4], passivity-based control [5] and other nonlinear approaches [6]. Furthermore, as quadrotors are used to material transportation, researchers have developed adaptive control algorithms to handle varying payloads [7]. By using reduced attitude, a nonlinear control algorithm is proposed in [8], where the authors validate the controller performance through both numerical simulations and experimental tests on a low-cost quadrotor platform. Finite-time control is reported in [9], although its application is limited to the attitude subsystem. Shi et al. [10] developed an almost global finite-time position and attitude control law for UAVs, leveraging the homogeneity framework to prove finite-time stability of the closed-loop system. Additionally, Sliding Mode Control (SMC) has been extensively used to achieve finite-time stability while simultaneously rejecting external disturbances [11]. To mitigate the chattering phenomena, a novel robust adaptive controller based on the super-twisting algorithm was developed in [12]. Nevertheless, that particular controller was designed based on the simplified model of the quadrotor dynamics, potentially limiting its performance in complex flight regimes. A saturated finite-time controller for quadrotors is reported in [13], although its application is limited to hovering maneuvers.

In finite-time controllers, the settling time required for the states to reach the equilibrium point depends on the initial conditions of the system. On the other hand, fixed-time stability introduced by Polyakov in the seminal work [14] ensures that the convergence time is bounded by a constant independent of the initial conditions. Fixed-time control algorithms utilizing state-dependent exponent coefficients for scalar and second-order systems subject to matched perturbations are presented in [15]. Furthermore, a recent singularity-free fixed-time controller based on SMC for robot manipulators was introduced in [16]. The previous works assume fully actuated systems. Wang et al. [17] developed a fixed-time rejection control strategy for quadrotors. To compensate for the external disturbance, the authors introduce an Extended State Observer (ESO) that achieve fixed-time convergence of the estimation errors. An output trajectory tracking controllers with input constraints based on fixed-time observer is proposed in [18].

Designing fixed-time control algorithms for QUAVs is a challenging task due to the under-actuated nature of the system, where the position and attitude subsystems are highly coupled, and the fact that attitude states evolve on a non-Euclidean manifold. In this paper, a solution is introduced for trajectory tracking of QUAVs. The attitude controller is designed based on the unit quaternion and hence is singularity free. Furthermore, the scheme is able to reject both matched and mismatched perturbations under some usual assumptions, e. g. they are bounded. The methodology is mainly based on the work in [19]–[21], and it effectively avoids any discontinuity at the origin, which yields to a bounded control output without the inclusion of a saturation function. Numerical simulations are consistent with the developed theory and show the

This work is supported by the **DGAPA–UNAM** under grant **IN103526**. The second and third authors acknowledge financial support from the CNRS through the MITI interdisciplinary programs through the exploratory research program and by the ANR agency under TROCOOL project (ANR-25-CE10-4393).

effectiveness and feasibility of the proposed control strategy.

The rest of the paper is organized as follows. Mathematical preliminaries regarding fixed-time stability and the general problem formulation are presented in Section II. The control strategy for QUAVs is introduced in Section III. Simulation results are reported in Section IV. The paper ends in Section V, which presents some concluding remarks.

II. GENERAL RESULTS

This section compiles some results about fixed-time stability and it introduces a new theorem.

A. Preliminaries

Lemma 2.1: [20] Consider the system

$$\dot{x} = -k\text{sign}(x)\,|x|^{\lambda\tanh(x^2)} + d(t) \qquad x(t_0) = x_0 \tag{1}$$

with $x(t) \in \mathbb{R}$, $\lambda > 0$, $d(t) \in \mathbb{R}$ an external perturbation such that $|d(t)| < \delta$ for a given $\delta > 0$. If

$$\lambda > \frac{\theta}{\tanh(1)} \qquad \theta > 1 \tag{2}$$

$$k > \frac{\delta}{\mu} > \delta \qquad \text{with} \qquad \mu = s_{\mathrm{m}}^{\lambda\tanh(s_{\mathrm{m}}^2)} < 1\,, \tag{3}$$

and $s_{\mathrm{m}} \approx 0.5829$ the solution of $\frac{\mathrm{d}}{\mathrm{d}x}\,|x|^{\lambda\tanh(x^2)}\Big|_{x=s_{\mathrm{m}}} = 0$, then the system is globally fixed-time stable and the settling-time satisfies

$$T(x_0) \le \frac{1}{(k-\delta)(\theta-1)} + \frac{1}{(k\,\mu-\delta)}\,. \tag{4}$$

$\triangle$

Lemma 2.2: [20], [21] Define

$$\tau(x,\lambda) = \text{sign}(x)\frac{\tanh(|x|^{\frac{1}{2}})}{\tanh(1)}|x|^{\frac{1}{2}\left(1-2\frac{\tanh(x^2)}{\tanh(1)}\right)}|x|^{\lambda\tanh(x^2)} \tag{5}$$

and consider the system

$$\dot{x}(t) = -k\,\tau(x(t),\lambda) + d(t) \qquad x(t_0) = x_0\,, \tag{6}$$

with $x(t) \in \mathbb{R}$, and $d(t) \in \mathbb{R}$ an external perturbation such that $|d(t)| < \delta$ for a given $\delta > 0$ and for all $t \ge t_0$. If

$$\lambda \ge \frac{\frac{1}{2}\theta + 1}{\tanh(1)}\,, \qquad \theta > 1 \tag{7}$$

$$k > \delta\frac{2}{\mu}\,, \tag{8}$$

with $\mu < 1$ given in (3), then $x(t), \dot{x}(t)$ remain bounded for all $t \ge t_0$, the system state satisfies $|x(t)| \le 1$ in a maximal fixed-time given by $T_1 \le \frac{2}{(k-\delta)(\theta-1)}$, and it becomes ultimately bounded by $|x(t)| \le a$ for an arbitrary small positive ultimate bound satisfying $a \le \frac{2\delta}{k\mu} < 1$, with a maximal settling-time given by $T_2 \le \frac{2|\ln(a)|}{k\mu}$. Moreover the derivative of $\tau(x(t),\lambda)$, which depends on $\dot{x}(t)$ explicitly (i. e. $\frac{\mathrm{d}}{\mathrm{d}t}\tau(x(t),\lambda) = \dot{\tau}(x(t),\dot{x}(t),\lambda)$), exists at $x(t) = 0$ for $\dot{x}(t) \ne 0$ and it satisfies $\dot{\tau}(0,0,\lambda) = 0$. Alternatively, the system is fixed-time stable with a maximal fixed-time given by

$$T_{\max} \le \frac{2}{(k-\delta)(\theta-1)} + \frac{g_\infty}{2k\mu}\,, \tag{9}$$

if from $t \ge t_0 + T_1$ it holds $d(t) = 0$, where g_∞ is a finite value given by

$$g(i) = \left(2^{\frac{1}{2^{i+1}}} - 1\right)\frac{2^{i+1}}{2^{\frac{i}{2^{i+1}}}} \quad \text{and} \quad g_\infty = \lim_{n\to\infty}\sum_{i=1}^{n} g(i)\,. \tag{10}$$

$\triangle$

Lemma 2.3: [21] Consider the function $\phi_\lambda(x) : \mathbb{R} \to \mathbb{R}$ given by

$$\phi_\lambda(x) = \frac{\tau(x,\lambda)}{2x} + \frac{|x|^{\left(\frac{\lambda\tanh(1)-1}{\tanh(1)}\right)\tanh(x^2)}}{2\tanh(1)\cosh^2(|x|^{\frac{1}{2}})} + \frac{\tau(x,\lambda)(\lambda\tanh(1)-1)\left\{2x^2\ln(|x|) + \tanh(x^2)\cosh^2(x^2)\right\}}{x\tanh(1)\cosh^2(x^2)}\,. \tag{11}$$

Then, with a proper choice of λ, it can always be guaranteed that

a) $\phi_\lambda(x)$ is singularity-free;
b) $\phi_\lambda(x) > 0$ for all $x \in \mathbb{R}$. $\triangle$

B. Fixed-time control for second order uncertain systems

Consider now the uncertain nonlinear second-order system

$$\dot{x}_1 = x_2 + d_1 \tag{12}$$

$$\dot{x}_2 = f(\boldsymbol{x}) + g(\boldsymbol{x})u + d_2\,, \tag{13}$$

with $\boldsymbol{x} = [x_1 \quad x_2]^{\mathrm{T}} \in \mathbb{R}^2$ the state, $u \in \mathbb{R}$ the control input, $f(\boldsymbol{x})$ and $g(\boldsymbol{x})$ continuous functions such that $f(\boldsymbol{0}) = 0$ and $g(\boldsymbol{x}) \ne 0$ for all $\boldsymbol{x} \in \mathbb{R}^2$, d_1 a mismatched disturbance such that $|d_1(t)| < \delta_1$ and d_2 a matched disturbance such that $|d_2(t)| < \delta_2$ for all $t \ge t_0$. Furthermore, it is assumed that d_1 is differentiable and $|\dot{d}_1(t)| < \bar{\delta}_1$ for all $t \ge t_0$.

Define the following sliding variable with a state-dependent exponent coefficient

$$s(t) = \dot{x}_1(t) + \beta(t)\,\tau(x_1(t),\lambda_{\mathrm{x1}}) \tag{14}$$

$$\beta(t) = (\beta_{\mathrm{M}} - \beta_{\mathrm{m}})\left(1 - e^{-\lambda(t-t_0)}\right) + \beta_{\mathrm{m}}\,, \tag{15}$$

where $\lambda > 0$, $\tau(x_1,\lambda_{\mathrm{x1}})$ is given as in (5), and

$$\beta_{\mathrm{M}} > \beta_{\mathrm{m}} > 0 \tag{16}$$

$$\lambda_{\mathrm{x1}} \ge \frac{\frac{1}{2}\theta_{\mathrm{x1}} + 1}{\tanh(1)}\,, \qquad \theta_{\mathrm{x1}} > 1\,. \tag{17}$$

By computing the derivative of (12) and substituting into (13) one gets

$$\ddot{x}_1 = f(\boldsymbol{x}) + g(\boldsymbol{x})u + \dot{d}_1 + d_2\,. \tag{18}$$

Then, since $|a|^b = \exp(b\ln(|a|))$, by direct calculation the derivative of s can be shown to satisfy:

$$\dot{s} = f(\boldsymbol{x}) + g(\boldsymbol{x})u + \dot{d}_1 + d_2 + \beta(t)\phi_\lambda(x_1)\dot{x}_1 + \dot{\beta}\tau\,. \tag{19}$$

The following control law is based on that given in [21]

$$
\begin{aligned}
u(\boldsymbol{x}) &= -g^{-1}(\boldsymbol{x})\left[f(\boldsymbol{x})+k_{\mathrm{s}}\mathrm{sign}(s)h(s)\right. \qquad (20)\\
&\qquad \left.+\beta(t)\phi_{\lambda}(x_1)(\dot{x}_1+k_{\mathrm{s}1}\mathrm{sign}(s))+\dot{\beta}\tau\right]\\
h(s) &= |s|^{\lambda_{\mathrm{s}}\tanh(s^2)}, \qquad (21)
\end{aligned}
$$

with $k_{\mathrm{s}1}, k_{\mathrm{s}}, \lambda_{\mathrm{s}} \in \mathbb{R}$ positive gains satisfying

$$
\lambda_{\mathrm{s}} > \frac{\theta_{\mathrm{s}}}{\tanh(1)}, \quad \theta_{\mathrm{s}} > 1 \qquad (22)
$$

$$
k_{\mathrm{s}1} > 0 \quad \text{and} \quad k_{\mathrm{s}} > \frac{\delta_{\mathrm{s}}}{\mu_{\mathrm{s}}}, \qquad (23)
$$

with $0 < \mu_{\mathrm{s}} < 1$ defined as in (3) and δ_{s} in (27).

Theorem 2.1: Consider system (12)-(13) in closed-loop with the control law (20). Then, a set of gains can always be found such that the following holds true:

a) The sliding variable $s(t)$ remains bounded for all $t \geq t_0$, and it becomes zero in a fixed-time $t_0 + T_{\mathrm{s}}$ given by

$$
\begin{aligned}
t_0 + T_{\mathrm{s}} &\leq t_0 + T_{\mathrm{s\,max}} \qquad (24)\\
&\leq t_0 + \frac{1}{(k_{\mathrm{s}}-\delta_{\mathrm{s}})(\theta_{\mathrm{s}}-1)} + \frac{1}{(k_{\mathrm{s}}\mu_{\mathrm{s}}-\delta_{\mathrm{s}})}.
\end{aligned}
$$

b) The states $x_1(t)$, $x_2(t)$ remain bounded for all $t \geq t_0$, and the state $x_1(t)$ becomes zero, i.e. $x_1(t) \equiv 0$, in a fixed-time no larger than

$$
t_0 + T_{\mathrm{e}} \leq t_0 + T_{\mathrm{smax}} + T_{\mathrm{e}1} + \frac{g_{\infty}}{2\beta_{\mathrm{e}}\mu_{\mathrm{x}1}}, \qquad (25)
$$

with $0 < \mu_{\mathrm{x}1} < 1$ as in (3), g_{∞} in (10), $\beta_{\mathrm{s}} = \beta(t_0 + T_{\mathrm{s}})$, $\beta_{\mathrm{e}} = \beta(t + T_{\mathrm{s}} + T_{\mathrm{e}1})$, and $T_{\mathrm{e}1} = \frac{2}{\beta_{\mathrm{s}}(\theta_{\mathrm{x}1}-1)}$.

Proof: The steps of the proof are:

a) Substitute the control law (20) in (19) to get

$$
\begin{aligned}
\dot{s} &= -k_{\mathrm{s}}\mathrm{sign}(s)|s|^{\lambda_{\mathrm{s}}\tanh(s^2)} + \dot{d}_1 + d_2 \qquad (26)\\
&\quad -k_{\mathrm{s}1}\mathrm{sign}(s)\beta(t)\phi_{\lambda}(x_1),
\end{aligned}
$$

where (21) has been used. Since according to Lemma 2.3 $\phi_{\lambda}(x_1) > 0$, the term $-k_{\mathrm{s}1}\beta(t)\phi_{\lambda}(x_1)\mathrm{sign}(s)$ always helps to yield s to the origin, so that in fact Lemma 2.1 can be directly employed to get $T_{\mathrm{s\,max}}$ in (24) by defining

$$
|\dot{d}_1 + d_2| \leq \bar{\delta}_1 + \delta_2 = \delta_{\mathrm{s}}. \qquad (27)
$$

Note that since $\dot{V} \leq 0$ for all $t \geq t_0$, then $s \in \mathcal{L}_{\infty}$.

b) The dynamics for x_1 satisfies from (14)

$$
\dot{x}_1 = -\beta(t)\,\tau(x_1(t), \lambda_{\mathrm{x}1}) + s(t). \qquad (28)
$$

It can be seen that this dynamics owns basically the form given in (6) because it has been shown that $s(t)$ is bounded for all time $t \geq t_0$, i.e. $|s(t)| \leq b_{\mathrm{s}}$ for $b_{\mathrm{s}} = |s(t_0)|$. However, Lemma 2.2 should not be used directly because this would force to have the condition $\beta_{\mathrm{m}} > b_{\mathrm{s}}\frac{2}{\mu}$ according to (8), which would make $\beta(t)$ dependent on the initial condition of $s(t)$. Instead, to prove only boundedness assume for simplicity's sake that $|x_1| \geq 1$ (because $|x_1| < 1$ is obviously bounded), and choose $V(x_1) = x_1^2$, whose derivative along (28) satisfies as worst possible situation

$$
\begin{aligned}
\dot{V} &\leq -2\beta_{\mathrm{m}}|\tau(x_1, \lambda_{\mathrm{x}1})||x_1| + 2|x_1|b_{\mathrm{s}} \qquad (29)\\
&= -2|x_1|(\beta_{\mathrm{m}}|\tau(x_1, \lambda_{\mathrm{x}1})| - b_{\mathrm{s}}),
\end{aligned}
$$

for all $t \geq t_0$. Assume that $\beta_{\mathrm{m}}|\tau(x_1, \lambda_{\mathrm{x}1})| - b_{\mathrm{s}} < 0$, so that $|x_1|$ is growing, and take into account that in view of definition (5) the function $|\tau(x_1, \lambda_{\mathrm{x}1})|$ is continuous, injective with respect to $|x_1|$ and increasing for $|x_1| \geq 1$. This means that there must exist a finite time $t_{\mathrm{x}} \geq t_0$ for which it is satisfied that $\beta_{\mathrm{m}}|\tau(x_1(t_{\mathrm{x}}), \lambda_{\mathrm{x}1})| - b_{\mathrm{s}} = 0$, so that $\dot{V} \equiv 0$, which implies that $|x_1|$ can no longer increase its value. On the contrary, if $\beta_{\mathrm{m}}|\tau(x_1, \lambda_{\mathrm{x}1})| - b_{\mathrm{s}} > 0$ then $\dot{V} < 0$ and $|x_1|$ is decreasing until once again one gets in a finite time $\beta_{\mathrm{m}}|\tau(x_1(t_{\mathrm{x}}), \lambda_{\mathrm{x}1})| - b_{\mathrm{s}} = 0$. Both situations imply that $x_1 \in \mathcal{L}_{\infty}$, which implicitly means that $\tau(x_1, \lambda_{\mathrm{x}1})$ remains bounded for all $t \geq t_0$.

From (28), the boundedness of x_1 implies that $\dot{x}_1$ remains bounded as well for all $t \geq t_0$, which in turn from (12) means that x_2 is bounded because d_1 is bounded by assumption. Then, since $f(\boldsymbol{x})$ and $g(\boldsymbol{x})$ are continuous by assumption, they are bounded for a bounded $\boldsymbol{x}$, while $h(s)$ is bounded by definition (21), which means from (20) that $u(\boldsymbol{x})$ is bounded as well because $\phi_{\lambda}(x_1)$ is bounded for a bounded x_1 and $\dot{\beta}$ is bounded by design. Finally, from (13) the boundedness of u implies that of $\dot{x}_2$ because d_2 is bounded by assumption.

Now, to show that x_1 becomes zero in fixed-time, recall that from $t \geq t_0 + T_{\mathrm{s}}$ the relationship (28) can be substituted by

$$
\dot{x}_1 = -\beta(t)\,\tau(x_1(t), \lambda_{\mathrm{x}1}), \qquad (30)
$$

which has basically the form given in (6) with $d(t) \equiv 0$ by considering that $\beta(t) \geq \beta_{\mathrm{m}}$. Therefore, Lemma 2.2 and the Comparison Lemma can be employed to get (25) by taking into account that $\beta(t) \geq \beta_{\mathrm{s}} = \beta(t + T_{\mathrm{s}})$ for all $t \geq t_0 + T_{\mathrm{s}}$ and $\beta(t) \geq \beta_{\mathrm{e}} = \beta(t + T_{\mathrm{s}} + T_{\mathrm{e}1})$ for all $t \geq t_0 + T_{\mathrm{s}} + T_{\mathrm{e}1}$, where $T_{\mathrm{e}1}$ stands for the time when $|x_1| \equiv 1$ is satisfied. Note that care should be taken in employing Lemma 2.2, since the time t_0 corresponds to the time $t_0 + T_{\mathrm{s\,max}}$ in this case. This concludes the proof. □

Remark 2.1: Usually, the derivative $\dot{x}_1$ is not available, but rather x_1 and x_2. This does not represent a drawback since an exact differentiator can be used for implementation [22]. △

III. Control of QUAVs

A. System model

The configuration of a QUAV is defined by the location of the center of mass and the attitude with respect to an inertial frame Σ_0. Therefore, the configuration manifold is the special Euclidean group $SE(3)$, which is the semidirect product of $\mathbb{R}^3$ and the special orthogonal group $SO(3) = \{{}^0\boldsymbol{R}_{\mathrm{b}} \in \mathbb{R}^{3\times3} \mid {}^0\boldsymbol{R}_{\mathrm{b}}^{\mathrm{T}}\,{}^0\boldsymbol{R}_{\mathrm{b}} = \boldsymbol{I}, \det{}^0\boldsymbol{R}_{\mathrm{b}} = 1\}$, where the subindex b stands for the body-fixed frame Σ_{b}. The translation equations of motion of the QUAV can be written as [2]

$$\dot{\boldsymbol{p}} = \boldsymbol{v} + \boldsymbol{d}_1 \qquad (31)$$

$$\dot{\boldsymbol{v}} = \frac{f}{m}\,{}^{0}\boldsymbol{R}_{\mathrm{b}}\,\boldsymbol{e}_3 - g\,\boldsymbol{e}_3 + \boldsymbol{d}_2\,, \qquad (32)$$

where $\boldsymbol{p} \in \mathbb{R}^3$ is the location of the center of mass in the inertial frame, $\boldsymbol{v} \in \mathbb{R}^3$ is the velocity of the center of mass in the inertial frame, $m \in \mathbb{R}$ is the total robot mass, $g = 9.81\mathrm{m/s^2}$ is the gravity of Earth, ${}^{0}\boldsymbol{R}_{\mathrm{b}}\,\boldsymbol{e}_3 \in \mathbb{R}^3$ denotes the direction of the total thrust with respect to the inertia frame, whose magnitude is given by $f \in \mathbb{R}$, $\boldsymbol{d}_1, \boldsymbol{d}_2 \in \mathbb{R}^3$ are external disturbances and $\boldsymbol{e}_1, \boldsymbol{e}_2, \boldsymbol{e}_3 \in \mathbb{R}^3$ are unitary vectors in the x, y, and z directions respectively[1].

The orientation dynamic equations are given by

$${}^{0}\dot{\boldsymbol{R}}_{\mathrm{b}} = = {}^{0}\boldsymbol{R}_{\mathrm{b}}\,\boldsymbol{S}\left({}^{\mathrm{b}}\boldsymbol{\omega}\right) \qquad (33)$$

$${}^{\mathrm{b}}\dot{\boldsymbol{\omega}} = \boldsymbol{M}^{-1}\boldsymbol{\tau} + \boldsymbol{M}^{-1}\boldsymbol{S}\left(\boldsymbol{M}\,{}^{\mathrm{b}}\boldsymbol{\omega}\right){}^{\mathrm{b}}\boldsymbol{\omega} + \boldsymbol{d}_3\,, \qquad (34)$$

where ${}^{\mathrm{b}}\boldsymbol{\omega} \in \mathbb{R}^3$ is the angular velocity expressed in the body-fixed frame Σ_{b}, $\boldsymbol{M} \in \mathbb{R}^{3\times 3}$ is the symmetric inertia matrix, $\boldsymbol{\tau} \in \mathbb{R}^3$ is the input torque, and $\boldsymbol{d}_3 \in \mathbb{R}^3$ is an external disturbance. The total thrust f and the input torque $\boldsymbol{\tau}$ are related to the angular velocities of the four rotors and in this work it is assumed that they can be freely chosen for simplicity.

B. Control design

Given a bounded desired pose $\boldsymbol{p}_{\mathrm{d}} \in \mathbb{R}^3$ for the QUAV, with at least bounded desired velocity $\boldsymbol{v}_{\mathrm{d}} = \dot{\boldsymbol{p}}_{\mathrm{d}} \in \mathbb{R}^3$, the corresponding errors for position and velocity are

$$\boldsymbol{e}_{\mathrm{p}} = \boldsymbol{p} - \boldsymbol{p}_{\mathrm{d}} \quad \text{and} \quad \boldsymbol{e}_{\mathrm{v}} = \boldsymbol{v} - \boldsymbol{v}_{\mathrm{d}}\,, \qquad (35)$$

respectively. System (31)-(32) owns basically the same structure as (12)-(13), but in vector form. However, the one single input of system (31)-(32) is the total thrust f, which makes it under-actuated. It order to solve this problem, recall that the rotation matrix ${}^{0}\boldsymbol{R}_{\mathrm{b}}$ represents the orientation of the body frame fixed at the center of the QUAV and which can be expressed as

$${}^{0}\boldsymbol{R}_{\mathrm{b}} = \left[\begin{array}{ccc} \boldsymbol{x}_{\mathrm{b}} & \boldsymbol{y}_{\mathrm{b}} & \boldsymbol{z}_{\mathrm{b}} \end{array}\right], \qquad (36)$$

where $\boldsymbol{x}_{\mathrm{b}}, \boldsymbol{y}_{\mathrm{b}}, \boldsymbol{z}_{\mathrm{b}} \in \mathbb{R}^3$ are unitary orthogonal directional vectors forming a dexterous coordinate system. Therefore, the product ${}^{0}\boldsymbol{R}_{\mathrm{b}}\,\boldsymbol{e}_3$ in (32) satisfies ${}^{0}\boldsymbol{R}_{\mathrm{b}}\,\boldsymbol{e}_3 = \boldsymbol{z}_{\mathrm{b}}$. A strategy design consists in using $\boldsymbol{z}_{\mathrm{b}}$ as an auxiliary control input by choosing its desired value $\boldsymbol{z}_{\mathrm{bd}} \in \mathbb{R}^3$ properly. In this way, $\boldsymbol{z}_{\mathrm{bd}}$ is given in terms of a desired input signal $\boldsymbol{u} \in \mathbb{R}^3$, i.e. $\boldsymbol{z}_{\mathrm{bd}} \in \mathbb{R}^3$ must satisfy

$$\boldsymbol{z}_{\mathrm{bd}} = \frac{1}{\|\boldsymbol{u}\|}\boldsymbol{u}\,, \qquad (37)$$

[1]The equations $\boldsymbol{v} = \dot{\boldsymbol{p}}$ and ${}^{0}\dot{\boldsymbol{R}}_{\mathrm{b}} = {}^{0}\boldsymbol{R}_{\mathrm{b}}\,\boldsymbol{S}({}^{\mathrm{b}}\boldsymbol{\omega})$ represent kinematic relationships and, therefore, there should not contain mismatched perturbations. However, since Theorem 2.1 states a general result, for the sake of completeness a mismatched disturbance is introduced artificially for the linear velocity as shown in (31).

where it can always be guaranteed that $\|\boldsymbol{u}\| \neq 0$ as long as the desired trajectory is properly defined according to physical constrains. By taking (37) into account, (32) can be rewritten as

$$\begin{aligned} \dot{\boldsymbol{v}} &= \frac{f}{m}\,{}^{0}\boldsymbol{R}_{\mathrm{b}}{}^{0}\boldsymbol{R}_{\mathrm{d}}^{\mathrm{T}}\,{}^{0}\boldsymbol{R}_{\mathrm{d}}\,\boldsymbol{e}_3 - g\,\boldsymbol{e}_3 + \boldsymbol{d}_2 \qquad (38)\\ &= \frac{f}{m}\,{}^{0}\boldsymbol{R}_{\mathrm{b}}{}^{0}\boldsymbol{R}_{\mathrm{d}}^{\mathrm{T}}\,\boldsymbol{z}_{\mathrm{bd}} - g\,\boldsymbol{e}_3 + \boldsymbol{d}_2\\ &= \frac{f}{m\|\boldsymbol{u}\|}\,{}^{0}\boldsymbol{R}_{\mathrm{b}}{}^{0}\boldsymbol{R}_{\mathrm{d}}^{\mathrm{T}}\,\boldsymbol{u} - g\,\boldsymbol{e}_3 + \boldsymbol{d}_2\,. \end{aligned}$$

Note that ${}^{0}\boldsymbol{R}_{\mathrm{b}} = {}^{0}\boldsymbol{R}_{\mathrm{d}}$ implies that ${}^{0}\boldsymbol{R}_{\mathrm{b}}{}^{0}\boldsymbol{R}_{\mathrm{d}}^{\mathrm{T}} = \boldsymbol{I}$, i.e. the identity matrix. Finally, by setting $f = m\|\boldsymbol{u}\|$ one gets

$$\dot{\boldsymbol{v}} = {}^{0}\boldsymbol{R}_{\mathrm{b}}{}^{0}\boldsymbol{R}_{\mathrm{d}}^{\mathrm{T}}\,\boldsymbol{u} - g\,\boldsymbol{e}_3 + \boldsymbol{d}_2\,.$$

A logical choice for $\boldsymbol{u}$ would be $\boldsymbol{u} = {}^{0}\boldsymbol{R}_{\mathrm{d}}{}^{0}\boldsymbol{R}_{\mathrm{b}}^{\mathrm{T}}\,\boldsymbol{u}_0$, with $\boldsymbol{u}_0 \in \mathbb{R}^3$ an auxiliary input vector. However, this would create an algebraic loop in the calculation of $\boldsymbol{u}$. Instead, it will be chosen

$$\boldsymbol{u} = {}^{0}\boldsymbol{R}_{\mathrm{df}}{}^{0}\boldsymbol{R}_{\mathrm{b}}^{\mathrm{T}}\,\boldsymbol{u}_0\,, \qquad (39)$$

where ${}^{0}\boldsymbol{R}_{\mathrm{df}} \in \mathbb{R}^{3\times 3}$ is the filtered desired attitude computed by using the delayed input $\boldsymbol{u}_{\mathrm{f}} \in \mathbb{R}^3$ given by

$$\dot{\boldsymbol{u}}_{\mathrm{f}} = -\gamma(\boldsymbol{u}_{\mathrm{f}} - \boldsymbol{u}) \quad \text{or} \quad \boldsymbol{U}_{\mathrm{f}}(s) = \frac{1}{\frac{1}{\gamma}s + 1}\boldsymbol{U}(s)\,, \qquad (40)$$

instead of $\boldsymbol{u}$, where $\gamma > 0$ is the cutoff frequency of the unitary gain filter. In doing so, one has $\overline{\boldsymbol{I}} = {}^{0}\boldsymbol{R}_{\mathrm{b}}{}^{0}\boldsymbol{R}_{\mathrm{d}}^{\mathrm{T}}{}^{0}\boldsymbol{R}_{\mathrm{df}}{}^{0}\boldsymbol{R}_{\mathrm{b}}^{\mathrm{T}}$. By choosing γ large enough then for low frequencies (with respect to the cutoff frequency γ) it is $\boldsymbol{u}_{\mathrm{f}} \approx \boldsymbol{u}$ because the filter gain is unitary, which in turn implies that one gets $\overline{\boldsymbol{I}} \approx {}^{0}\boldsymbol{R}_{\mathrm{b}}{}^{0}\boldsymbol{R}_{\mathrm{d}}^{\mathrm{T}}{}^{0}\boldsymbol{R}_{\mathrm{d}}{}^{0}\boldsymbol{R}_{\mathrm{b}}^{\mathrm{T}} = \boldsymbol{I}$ because ${}^{0}\boldsymbol{R}_{\mathrm{df}} \approx {}^{0}\boldsymbol{R}_{\mathrm{d}}$. $\boldsymbol{x}_{\mathrm{bd}}$ and $\boldsymbol{y}_{\mathrm{bd}}$, along with the desired angular velocity $\boldsymbol{\omega}_{\mathrm{d}} \in \mathbb{R}^3$, are obtained according to the method proposed in [23]. Finally, one gets the equivalent dynamics

$$\dot{\boldsymbol{v}} = \overline{\boldsymbol{I}}\boldsymbol{u}_0 - g\,\boldsymbol{e}_3 + \boldsymbol{d}_2\,. \qquad (41)$$

This will allow the design of the control law $\boldsymbol{u}_0$ directly by using Theorem 2.1, since system (31) and (41) can now be rewritten in terms of tracking errors as

$$\dot{\boldsymbol{e}}_{\mathrm{p}} = \dot{\boldsymbol{p}} - \dot{\boldsymbol{p}}_{\mathrm{d}} = \boldsymbol{v} - \boldsymbol{v}_{\mathrm{d}} + \boldsymbol{d}_1 = \boldsymbol{e}_{\mathrm{v}} + \boldsymbol{d}_1 \qquad (42)$$

$$\dot{\boldsymbol{e}}_{\mathrm{v}} = \dot{\boldsymbol{v}} - \dot{\boldsymbol{v}}_{\mathrm{d}} = \overline{\boldsymbol{I}}\boldsymbol{u}_0 - g\,\boldsymbol{e}_3 + \boldsymbol{d}_2 - \dot{\boldsymbol{v}}_{\mathrm{d}}\,. \qquad (43)$$

The error system (42)-(43) represents three decoupled subsystems of the form (12)-(13), which allows to apply directly the results of Section III. From (14) and (20), the components of the auxiliary control $\boldsymbol{u}_0$ takes the following form

$$\begin{aligned} u_{0i} = \boldsymbol{e}_i^{\mathrm{T}}\boldsymbol{u}_0 =& \boldsymbol{e}_i^{\mathrm{T}} g\boldsymbol{e}_3 - k_{\mathrm{s}i}\mathrm{sign}(\boldsymbol{e}_i^{\mathrm{T}}\boldsymbol{s})h(\boldsymbol{e}_i^{\mathrm{T}}\boldsymbol{s}) - \dot{\beta}\tau(\boldsymbol{e}_i^{\mathrm{T}}\boldsymbol{e}_{\mathrm{p}})\\ &- \beta\phi_{\lambda}(\boldsymbol{e}_i^{\mathrm{T}}\boldsymbol{e}_{\mathrm{p}})\left(\boldsymbol{e}_i^{\mathrm{T}}\dot{\boldsymbol{e}}_{\mathrm{p}} + k_{\mathrm{s}1}\mathrm{sign}(\boldsymbol{e}_i^{\mathrm{T}}\boldsymbol{s})\right) \qquad (44) \end{aligned}$$

where u_{0i} is the i-th element of $\boldsymbol{u}_0$, $\boldsymbol{e}_i^{\mathrm{T}}\boldsymbol{s} = \boldsymbol{e}_i^{\mathrm{T}}\dot{\boldsymbol{e}}_{\mathrm{p}} + \beta(t)\tau(\boldsymbol{e}_i^{\mathrm{T}}\boldsymbol{e}_{\mathrm{p}}, \lambda_{\mathrm{x}1})$ with $i = 1, 2, 3$. However, it remains to guarantee that $\boldsymbol{z}_{\mathrm{b}} = \boldsymbol{z}_{\mathrm{bd}}$. Therefore, the next step is to design

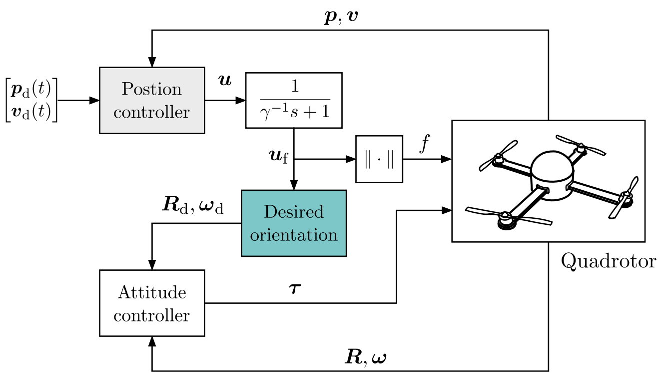

Fig. 1. Block diagram of the position and attitude control laws

a tracking controller for subsystem (33)-(34). To this goal, consider the attitude and angular velocity errors defined as

$$\boldsymbol{R}_{\mathrm{e}} = {}^0\boldsymbol{R}_{\mathrm{d}}^{\mathrm{T}}\,{}^0\boldsymbol{R}_{\mathrm{b}} = {}^{\mathrm{d}}\boldsymbol{R}_0\,{}^0\boldsymbol{R}_{\mathrm{b}} \quad (45)$$

$$\boldsymbol{e}_\omega = {}^{\mathrm{b}}\boldsymbol{\omega} - \boldsymbol{R}_{\mathrm{e}}^{\mathrm{T}}\boldsymbol{\omega}_{\mathrm{d}}\,. \quad (46)$$

In addition, consider the unit quaternion $\mathcal{Q}\left({}^{\mathrm{d}}\eta_{\mathrm{b}}, {}^{\mathrm{d}}\boldsymbol{\varepsilon}_{\mathrm{b}}\right)$ associated to the rotation matrix $\boldsymbol{R}_{\mathrm{e}} \in SO(3)$, where ${}^{\mathrm{d}}\eta_{\mathrm{b}} \in \mathbb{R}$ is the scalar part and ${}^{\mathrm{d}}\boldsymbol{\varepsilon}_{\mathrm{b}} \in \mathbb{R}^3$ is the vector part. The following identities hold [24]

$${}^0\dot{\boldsymbol{R}}_{\mathrm{d}} = {}^0\boldsymbol{R}_{\mathrm{d}}\boldsymbol{S}\left(\boldsymbol{\omega}_{\mathrm{d}}\right) \quad (47)$$

$${}^{\mathrm{d}}\dot{\eta}_{\mathrm{b}} = -\frac{1}{2}\,{}^{\mathrm{d}}\boldsymbol{\varepsilon}_{\mathrm{b}}^{\mathrm{T}}\,\boldsymbol{e}_\omega \quad (48)$$

$${}^{\mathrm{d}}\dot{\boldsymbol{\varepsilon}}_{\mathrm{b}} = \frac{1}{2}\left({}^{\mathrm{d}}\eta_{\mathrm{b}}\,\boldsymbol{I} + \boldsymbol{S}\left({}^{\mathrm{d}}\boldsymbol{\varepsilon}_{\mathrm{b}}\right)\right)\boldsymbol{e}_\omega\,, \quad (49)$$

where $\boldsymbol{\omega}_{\mathrm{d}} \in \mathbb{R}^3$ is the desired angular velocity expressed in the desired frame Σ_{d}. Based on this, define

$$\boldsymbol{s}_\omega = \boldsymbol{e}_\omega + k_\epsilon\,{}^{\mathrm{d}}\boldsymbol{\varepsilon}_{\mathrm{b}}\,, \quad (50)$$

where k_ϵ is a positive scalar constant. Define

$$\boldsymbol{\tau} = \boldsymbol{M}\left(\boldsymbol{R}_{\mathrm{e}}^{\mathrm{T}}\dot{\boldsymbol{\omega}}_{\mathrm{d}} - \boldsymbol{S}\left({}^{\mathrm{b}}\boldsymbol{\omega}\right)\boldsymbol{R}_{\mathrm{e}}^{\mathrm{T}}\boldsymbol{\omega}_{\mathrm{d}} - \boldsymbol{K}_0\boldsymbol{\tau}_0 - \frac{1}{2}k_\epsilon\left({}^{\mathrm{d}}\eta_{\mathrm{b}}\,\boldsymbol{I} + \boldsymbol{S}\left({}^{\mathrm{d}}\boldsymbol{\varepsilon}_{\mathrm{b}}\right)\right)\boldsymbol{e}_\omega\right) - \boldsymbol{S}\left(\boldsymbol{M}\,{}^{\mathrm{b}}\boldsymbol{\omega}\right){}^{\mathrm{b}}\boldsymbol{\omega}\,, \quad (51)$$

where $\boldsymbol{K}_0 \in \mathbb{R}^{3\times3}$ is a diagonal positive definite matrix and $\boldsymbol{\tau}_0 \in \mathbb{R}^3$ is an auxiliary control input whose elements are

$$\tau_{0i} = \boldsymbol{e}_i^{\mathrm{T}}\boldsymbol{\tau}_0 = \tau(\boldsymbol{e}_i^{\mathrm{T}}\boldsymbol{s}_\omega, \lambda), \quad i = 1, 2, 3. \quad (52)$$

By substituting (51) in (34) delivers the following dynamics

$$\dot{\boldsymbol{s}}_\omega = -\boldsymbol{K}_0\boldsymbol{\tau}_0 + \boldsymbol{d}_3\,. \quad (53)$$

This relationship represents three decoupled dynamic equations for $\boldsymbol{s}_\omega$ which own the form given by (6), so that the result of Lemma 2.2 can be used directly. Once $\boldsymbol{s}_\omega \equiv \boldsymbol{0}$ is satisfied it can be shown that $\boldsymbol{e}_\omega = \boldsymbol{0}$ and ${}^0\boldsymbol{R}_{\mathrm{b}} = {}^0\boldsymbol{R}_{\mathrm{d}}$ asymptotically [24]. A block diagram of the control strategy is depicted in Figure 1.

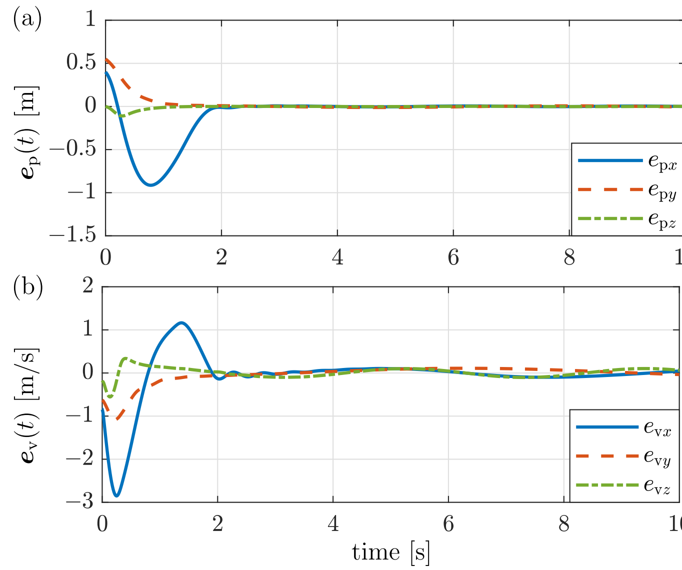

Fig. 2. Time evolution of the position and velocity tracking errors. a) Position error $\boldsymbol{e}_{\mathrm{p}}(t)$m. b) Velocity error $\boldsymbol{e}_{\mathrm{v}}(t)$m/s

IV. Simulation results

Assume that the system outputs $\boldsymbol{x}_1 = \boldsymbol{p}$ and $\boldsymbol{x}_2 = \boldsymbol{v}$ are free of noise, while $\dot{\boldsymbol{e}}_{\mathrm{p}}$ is obtained by using a differentiator similar to that given in [22] (omitted here for lack of space). To assess the performance of the proposed control strategy, a simulation study is conducted, where the aerial robot parameters $m = 4.34$Kg and $\boldsymbol{M} = \mathrm{diag}(0.0820, 0.0845, 0.1377)$ Kg·m^2 reported in [25] are used. The control parameters for the position control are set as $\lambda_{\mathrm{x}1} = 3$, $\lambda_{\mathrm{s}} = 3$, $k_{\mathrm{s}1} = 0.1$ and $\boldsymbol{K}_{\mathrm{s}} = \mathrm{diag}(1.5, 1.5, 1.5)$, while the attitude control gains are chosen as $\lambda_\omega = 3$, $k_{\mathrm{e}} = 15$, $\gamma = 15$ and $\boldsymbol{K}_0 = \mathrm{diag}(67.5, 45, 45)$. The desired position trajectory is given by $\boldsymbol{p}_{\mathrm{d}}(t) = \mathrm{diag}\{0.4\sin(\frac{2\pi t}{3})\,, 0.6\sin(\frac{2\pi t}{6})\,, 0.4(1 - \exp(-0.75t))\}$m, which represents a lemniscate curve in the (x-y) plane. The initial condition of the robot is selected as $\boldsymbol{p}(0) = \begin{bmatrix} 0.4 & 0.55 & 0 \end{bmatrix}^{\mathrm{T}}$m, $\boldsymbol{v}(0) = \boldsymbol{0}$, $\mathcal{Q} = (1, \boldsymbol{0})$ and $\boldsymbol{\omega}(0) = \boldsymbol{0}$. Also, the following time-varying disturbances are included: $\boldsymbol{d}_1 = 0.1\mathrm{diag}\{\sin(t)\,, \cos(0.5t)\,, -\sin(1.5t)\}$ m/s, $\boldsymbol{d}_2 = \mathrm{diag}\{0.1 + 0.2\cos(t-2)\,, -0.2 + \sin(t)\,, 0.15(1 - \exp(-t))\cos(2t)\}$N, $\boldsymbol{d}_3 = \mathrm{diag}\{0.1 + 0.3\sin(t/6)\,, -0.3\,, -0.15 + 0.3\sin(t/6)\}$Nm. The time evolution of the position error $\boldsymbol{e}_{\mathrm{p}}(t)$ and velocity error $\boldsymbol{e}_{\mathrm{v}}(t)$ are shown in Figure 2. The figure shows that the aerial robot achieves trajectory tracking in less than 3s even in the presence of non-vanishing time-varying disturbances. The time evolution of the attitude and angular velocity errors are shown in Figures 3 and 4, respectively. Note that $\boldsymbol{e}_{\mathrm{v}}$ does not vanish completely because of the presence of $\boldsymbol{d}_1$, but its magnitude tends to be $-\boldsymbol{d}_1$ [19]. The attitude control gains were selected such that the attitude subsystem responds faster than the position subsystem. The numerical results demonstrate the trajectory tracking capability and robustness of the proposed control framework.

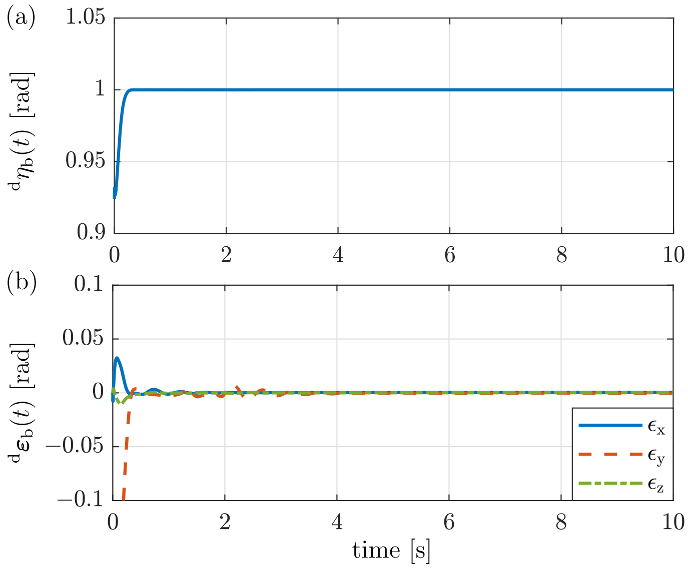

Fig. 3. Time evolution of the attitude error $\mathcal{Q}(t)$. a) Scalar part $\eta_{\mathrm{b}}(t)$. b) Vector part $\boldsymbol{\epsilon}_{\mathrm{b}}(t)$.

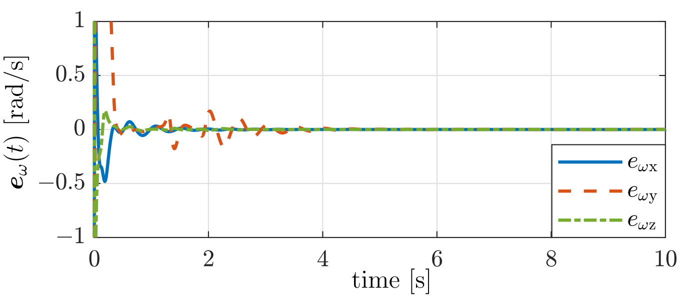

Fig. 4. Time evolution of the angular velocity error $\boldsymbol{\omega}_{\mathrm{e}}(t)$rad/s

V. Conclusions

This contribution introduces a sliding mode fixed-time controller for trajectory position tracking of Quadrotor Unmanned Aerial Vehicles (QUAVs). The approach is based on using the desired orientation as an input for the under actuated position system. For the fixed-time stabilization, a new theorem is introduced which proposes a control law able to reject matched and mismatched perturbations for a class of nonlinear systems, and then it is shown how this result can be employed for the QUAVs. The approach is tested satisfactory by means of a simulation. As future work it remains to carry out an experimental study.

References

[1] A. Rejeb, K. Rejeb, S. J. Simske, and H. Treiblmaier, "Drones for supply chain management and logistics: a review and research agenda," *International Journal of Logistics Research and Applications*, vol. 26, no. 6, pp. 708–731, Sept. 2021.

[2] R. Mahony, V. Kumar, and P. Corke, "Multirotor aerial vehicles: Modeling, estimation, and control of quadrotor," *IEEE Robotics and Automation Magazine*, vol. 19, no. 3, pp. 20–32, Sept. 2012.

[3] I. Lopez-Sanchez and J. Moreno-Valenzuela, "Pid control of quadrotor uavs: A survey," *Annual Reviews in Control*, vol. 56, p. 100900, 2023.

[4] A.-W. A. Saif, A. Aliyu, M. A. Dhaifallah, and M. Elshafei, "Decentralized backstepping control of a quadrotor with tilted-rotor under wind gusts," *International Journal of Control, Automation and Systems*, vol. 16, no. 5, pp. 2458–2472, Sept. 2018.

[5] J. R. Montoya-Morales, M. E. Guerrero-Sánchez, G. Valencia-Palomo, O. Hernández-González, F. R. López-Estrada, and L. C. Félix-Herrán, "Design and experimental validation of ida-pbc-based flight control for quadrotors," *Robotica*, vol. 43, no. 7, pp. 2376–2397, June 2025.

[6] J. Moreno-Valenzuela, R. Perez-Alcocer, M. Guerrero-Medina, and A. Dzul, "Nonlinear pid-type controller for quadrotor trajectory tracking," *IEEE/ASME Transactions on Mechatronics*, vol. 23, no. 5, pp. 2436–2447, Oct. 2018.

[7] L. Kong, W. He, and C. Silvestre, "A two-layer adaptive control framework for prescribed performance in unmanned aerial vehicles," *Automatica*, vol. 185, p. 112783, Mar. 2026.

[8] C. Montañez-Molina and J. Pliego-Jiménez, "Position and reduced attitude trajectory tracking control of quadrotors: Theory and experiments," *Aerospace Science and Technology*, vol. 155, p. 109683, Dec. 2024.

[9] Y. Ju and G. Diao, "Virtual finite time control of quadrotor unmanned aerial vehicle based on set stability," *Journal of The Franklin Institute*, vol. 362, no. 1, p. 107451, Jan. 2025.

[10] X.-N. Shi, Y.-A. Zhang, and D. Zhou, "Almost-global finite-time trajectory tracking control for quadrotors in the exponential coordinates," *IEEE Transactions on Aerospace and Electronic Systems*, vol. 53, no. 1, pp. 91–100, 2017.

[11] M. M. Fatemi and A. Akbarimajd, "Adaptive sliding mode control for quadrotor uavs under disturbances using multi-layer perceptron," *IEEE Access*, vol. 13, pp. 45 518–45 526, 2025.

[12] C. Rosales, C. Vacca Sisterna, F. Rossomando, D. Gandolfo, C. Soria, and R. Carelli, "Super-twisting adaptive control of a quadrotor," *ISA Transactions*, vol. 166, pp. 241–249, Nov. 2025.

[13] W. Zhu, H. Du, Y. Cheng, and Z. Chu, "Hovering control for quadrotor aircraft based on finite-time control algorithm," *Nonlinear Dynamics*, vol. 88, no. 4, pp. 2359–2369, Feb. 2017.

[14] A. Polyakov, "Nonlinear feedback design for fixed-time stabilization of linear control systems," *IEEE Transactions on Automatic Control*, vol. 57, no. 8, pp. 2106–2110, 2012.

[15] E. Moulay, V. Léchappé, E. Bernuau, and F. Plestan, "Robust fixed-time stability: Application to sliding-mode control," *IEEE Transactions on Automatic Control*, vol. 67, no. 2, pp. 1061–1066, 2022.

[16] M. A. Arteaga, E. Moulay, and M. Defoort, "A robust nonsingular fixed-time controller: Application to robot manipulators," *Journal of The Franklin Institute*, vol. 362, no. 18, p. 108216, 2025.

[17] T. Wang, Y. Xia, K. Zhao, W. Ning, and W. Zhao, "Fixed-time disturbance rejection control scheme for quadrotor trajectory tracking," *IEEE Transactions on Industrial Electronics*, vol. 72, no. 11, pp. 11 671–11 681, Nov. 2025.

[18] Y. Xia, M. Gong, D. Ma, and G. Shen, "Saturated output feedback control for quadrotor trajectory tracking via fixed-time observers," *Control Engineering Practice*, vol. 168, p. 106713, Mar. 2026.

[19] E. Moulay, V. Léchappé, E. Bernuau, M. Defoort, and F. Plestan, "Fixed-time sliding mode control with mismatched disturbances," *Automatica*, vol. 136, p. 110009, 2022.

[20] M. A. Arteaga, E. Moulay, and M. Defoort, "A nonsingular fixed-time sliding mode controller for robot manipulators in the presence of external perturbations and partially known model," *International Journal of Robust and Nonlinear Control*, vol. 25, pp. 2010–2026, 2025.

[21] ——, "A robust sliding mode controller for nonlinear systems with mismatched perturbations," in *2025 European Control Conference (ECC)*. Thessaloniki, Greece: European Control Conference, June 2025, pp. 1225–1230.

[22] A. Levant and M. Livne, "Globally convergent differentiators with variable gains," *International Journal of Control*, vol. 91, no. 9, pp. 1994–2008, 2018.

[23] J. Pliego-Jiménez, "Quaternion-based adaptive control for trajectory tracking of quadrotor unmanned aerial vehicles," *International Journal of Adaptive Control and Signal Processing*, vol. 35, no. 5, pp. 628–641, Feb. 2021.

[24] M. A. Arteaga, A. Gutiérrez-Giles, and J. Pliego-Jiménez, *Local Stability and Ultimate Boundedness in the Control of Robot Manipulators*. Cham, Switzerland: Springer, 2022.

[25] T. Lee, M. Leok, and N. H. McClamroch, "Geometric tracking control of a quadrotor uav on se(3)," in *49th IEEE Conference on Decision and Control (CDC)*. IEEE, Dec. 2010, pp. 5420–5425.